DOI: 10.1002/zaac.200800097

1,4,6,9-Tetraoxa-5λ^4-selena-spiro[4.4]nonane − A Combined Theoretical and Experimental Study

Richard Betz, Maximilian Pfister, Moritz M. Reichvilser, and Peter Klüfers*

München, Ludwig-Maximilians-Universität, Department Chemie und Biochemie

Received March 12th, 2008.

Dedicated to Professor Heinrich Nöth on the Occasion of his 80th Birthday

Abstract. The symmetric *spiro*-selenurane derived from ethylene glycol, 1,4,6,9-tetraoxa-5λ^4-selena-spiro[4.4]nonane, was prepared from selenium tetrachloride and ethylene glycol and its molecular structure was determined by single crystal X-ray diffraction. NBO analyses for the title compound and a related compound were conducted to assess the role of the stereochemical active lone pair on the selenium atom on the structure.

Keywords: Selenium; Structure elucidation; Density functional calculations; NBO analysis; Bond theory

Introduction

The structure and bonding of tetracoordinate selenium compounds is a significant issue in bonding theory. According to the diagonal relationship between phosphorus and selenium, the chemistry of these compounds bears an interesting feature when considering the evidence for the transitional pentavalency of phosphorus in the course of phosphotransferyl reactions or the hydrolysis of esters of orthophosphoric acid *in vivo* [1−3]. Higher oxidation states of selenium, which is known to be an essential element for the reproductive capability of many organisms [4], may be intermediates in the metabolism of this element. Polyols and carbohydrates offering various bonding sites with their oxygen donor functions appear to be reasonable bonding partners for selenium in living organisms. However, this area of selenium chemistry requires further investigation.

The simplest symmetric *spiro*-selenurane derived from a vicinal diol was first prepared by *Paetzold* and *Reichenbächer* from selenium tetrachloride and ethylene glycol and later by *Denney* et al. by the same synthetic approach [5, 6]. As of today, the molecular structure of this compound, $Se(C_2H_4O_2)_2$ (**1**), has not been elucidated by means of single crystal X-ray analysis. However, the crystal structure of a similar compound applying pinacol as the chelating diol, $Se(C_6H_{12}O_2)_2$ (**2**), was published by *Day* and *Holmes* [7]. These authors assigned the detected pseudo-trigonal-bipyramidal coordination polyhedron around the selenium atom to the presence of a stereochemical active lone pair at the selenium(IV) center. In a program to develop a carbohydrate chemistry of the non-metallic p-block elements, we succeeded in the crystallization of the parent compound **1**. We thus report herein the molecular parameters of this *spiro*-selenurane and interpret the structure in light of a computer-chemical analysis using the natural-bond-orbital (NBO) approach. The compound is also characterized by means of melting point measurement, NMR, IR, Raman, UV/Vis, and mass spectrometry as well as elemental analyses.

Experimental Section

General Aspects

Selenium tetrachloride was obtained from Aldrich (reagent grade) and used without further purification. Ethylene glycol (reagent grade) was supplied by Fluka and dried over molecular sieves (3 Å). Tetrahydrofuran (reagent grade) was obtained from Fluka and dried over molecular sieves (4 Å). Triethylamine (reagent grade) was obtained from Riedel-de-Haën and stored over potassium hydroxide pellets prior to use. A detailed description of the experimental procedure is given due to the partial and scarce descriptions in the literature.

Physical measurements

^{1}H NMR spectra were measured with a Jeol Eclipse 400 spectrometer at 400 MHz and are referenced to internal tetramethylsilane. ^{13}C NMR spectra were measured with a Jeol Eclipse 400 spectrometer at 101 MHz and are referenced to internal tetramethylsilane. ^{77}Se NMR spectra were recorded with a Jeol Eclipse 400 spectrometer at 76 MHz and are referenced to external dimethylselan. Mass spectra were recorded with a JEOL JMS-700 spectrometer. IR spectra were recorded with a Perkin Elmer Spectrum BX FT-IR spectrometer with a DuraSamplIR II ATR unit. Raman spectra were measured with a Perkin Elmer 2000 NIR-FT spectrometer. UV/VIS spectra were measured with a CARY 50 Bio UV-

* Prof. Dr. Peter Klüfers
Department Chemie und Biochemie der Ludwig-Maximilians-Universität München
Butenandtstr. 5−13
D-81377 München, Germany
E-mail: kluef@cup.uni-muenchen.de

Visible spectrometer in quartz glass cuvettes. Elemental analysis was done on a Vario Elementar EL apparatus. The content of selenium was determined by ICP-AES on a Varian-VISTA Simultan spectrometer. The melting point was obtained on a Büchi-540 apparatus and is uncorrected.

DFT calculations and NBO analyses

The geometries of **1** and **2** were optimized with Gaussian03 [8] at the B3LYP/6-31+G(2d,p) level of theory with very tight convergence criteria and an ultrafine integration grid. Frequency analyses were performed to ensure that the obtained geometries represent minima on the potential energy hypersurface. The bonding situation was investigated by means of natural bond orbital analyses [9].

Crystallography

Intensity data were collected using an Oxford XCalibur 3 diffractometer (Mo-Kα radiation, λ = 0.71073 Å) at 200 K. The structure was solved using the program SIR-97 [10] and refined with SHELXL-97 [11]. The molecular diagram was prepared with ORTEP III [12].

Preparation of 1,4,6,9-Tetraoxa-5λ⁴-selena-spiro[4.4]nonane, $Se(C_2H_4O_2)_2$ (1)

A three-necked flask (500 mL) equipped with two dropping funnels and a pressure equalizing valve was charged under nitrogen with selenium tetrachloride (7.15 g, 32.4 mmol) and tetrahydrofuran (155 mL). After the complete dissolution of selenium tetrachloride, ethylene glycol (3.61 mL, 4.02 g, 64.8 mmol) was added dropwise over 10 minutes. After the addition was completed, the reaction mixture was cooled to −40 °C and a solution of triethylamine (18.06 mL, 13.15 g, 130 mmol) in tetrahydrofuran (65 mL) was added over the course of 30 minutes. A heavy, colorless solid separated from the reaction mixture immediately. The colorless suspension was then stirred for another 30 minutes with persistent cooling, separated from the solid by filtration under nitrogen and concentrated to approximately one fifth of its volume under reduced pressure. Upon storage at −25 °C colorless platelets were obtained, yield 2.44 g, 12.3 mmol, 38.0 %. Melting point: 99.2−101.7 °C (lit.: 102 °C [5]).Elemental analysis found (calculated for $C_4H_8O_4Se$): C 23.80 % (24.13 %), H 4.13 % (4.05 %).

^{1}H NMR ($CDCl_3$, 399.8 MHz, 21 °C): δ = 4.18−4.11 (m, 4 H, CH_2), 4.00−3.93 (m, 4 H, CH_2). **^{13}C NMR** ($CDCl_3$, 100.5 MHz, 23 °C): δ = 65.4 (CH_2). **^{77}Se NMR** ($CDCl_3$, 76.2 MHz, 23 °C): δ = 1255. **ICP-AES**, found (calculated for $C_4H_8O_4Se$): Se 43.84 % (39.67 %); sensitivity of compound against hydrolysis hampered preparation of sample. **MS** (CI+, isobutane): 201 ($[M+H]^+$). **IR** (neat): ν = 2990 (w, CH_2), 2952 (m, CH_2), 2936 (m, CH_2), 2878 (s, CH_2), 1465 (w), 1357 (w), 1336 (w), 1324 (w), 1220 (m), 1212 (m), 1120 (m), 1089 (w), 1044 (m), 1023 (s), 908 (s), 892 (m), 880 (m) cm^{-1}. **Raman** (neat): ν = 2992 (39, CH_2), 2981 (25, CH_2), 2965 (43, CH_2), 2880 (35, CH_2), 1469 (20), 1460 (17), 1366 (9), 1337 (5), 1215 (14), 1120 (6), 1002 (7), 922 (18), 887 (6), 649 (58), 640 (55), 605 (100), 586 (22), 493 (8), 471 (28), 439 (50), 430 (74), 348 (14), 290 (5), 192 (3), 160 (5) cm^{-1}. **UV/Vis** (acetonitril): 220.0 nm; **UV/Vis** (cyclohexane): 219.1 nm.

Crystal structure determination

1: $C_4H_8O_4Se$, M_r = 199.06 g mol^{-1}, colorless block, 0.28 × 0.19 × 0.18 mm, monoclinic, $P2_1/c$, a = 7.908(5), b = 6.670(5), c = 13.218(5) Å, β = 114.33(2)°, V = 635.3(7) Å^3, Z = 4, ρ = 2.081 g cm^{-3}, T = 200(2) K, μ(MoKα) = 5.850 mm^{-1}, numerical absorption correction, Oxford XCalibur 3, MoKα radiation (λ = 0.71073 Å), θ range = 4.03−27.57°, 3513 refls., 1463 independent and used in refinement, 1006 with $I \geq 2\sigma(I)$, R_{int} = 0.0319, mean $\sigma(I)/I$ = 0.0359, 83 parameters, $R(F_{obs})$ = 0.0287, $R_w(F^2)$ = 0.0743, S = 0.975, min. and max. residual electron density: −0.908/0.473 e Å^{-3}, max. shift/error = 0.001.

Crystallographic data have been deposited with the Cambridge Crystallographic Data Centre as supplementary publication CCDC-656365. Copies of the data can be obtained free of charge on application to CCDC, 12 Union Road, Cambridge CB2 1EZ, UK (Fax: int.code+(1223)336-033; e-mail for inquiry: file-server@ccdc.cam.ac.uk).

Results and Discussion

Crystal structure analysis

The title compound was prepared according to the procedure outlined by *Paetzold* and *Reichenbächer* in a one-step procedure upon the reaction of selenium tetrachloride and ethylene glycol [5]. The results of a single-crystal X-ray study show the selenium atom as the center of a *spiro* compound (Figure 1). The seesaw-shaped molecules show axial Se-O distances that are slightly longer than the corresponding distances in the equatorial plane (for selected average bond lengths and angles see Table 1). The values for Se-O distances in **1** are similar to those observed for the pinacol-derived *spiro*-selenurane $Se(C_6H_{12}O_2)_2$ (**2**) [7]. Small differences are observed for the O_{ax}-Se-O_{ax} angle − which is closer to linearity in **1** − and the O_{eq}-Se-O_{eq} angle, which

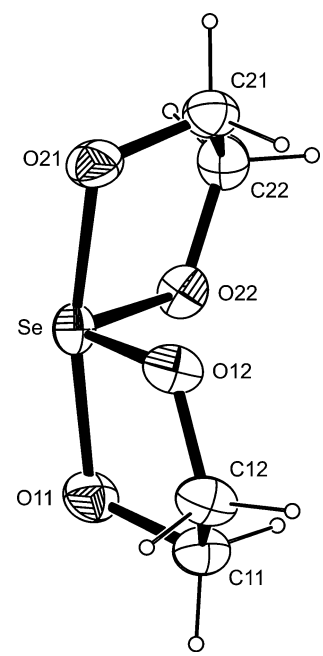

Figure 1 Structure of $Se(C_2H_4O_2)_2$ (**1**) (50 % probability ellipsoids). For selected average bond lengths and angles cf. Table 1. Selected individual bond lengths (in Å) and angles (in °): Se-O11 1.874(2), Se-O12 1.780(2), Se-O21 1.863(2), Se-O22 1.791(2), O21-Se-O11 167.8(1), O12-Se-O22 103.9(1).

deviates more from 120° than the corresponding angle in **2**. Both five-membered rings adopt an *envelope* conformation (ring puckering analysis [13]: Se-O11-C11-C12-O12: Q_2 = 0.384(4) Å, φ_2 = 252.4(4)°, *envelope* on C11; Se-O21-C21-C22-O22: Q_2 = 0.384(4) Å, φ_2 = 250.6(4)°, *envelope* on C21.)

NMR properties and hydrolytic stability

^{13}C NMR spectra of dissolved crystals of **1** in $CDCl_3$ show only one resonance. A comparison with the chemical shift of pure ethylene glycol in the same solvent shows that upon bonding to selenium the carbon resonances are shifted about 1.7 ppm downfield. ^{1}H NMR spectra of the same sample showed a complex but symmetric multiplet pattern. The downfield shift for the protons in comparison to neat ethylene glycol ranks from 0.22 to 0.47 ppm.

1 is rather unstable against hydrolysis and quickly decomposes in solution and in the solid state: when exposed to air, crystals of **1** lose their brilliance and deliquesce within minutes. Simultaneously, a gradually intensifying reddish color and a garlic-like odor appear. When a sample was exposed to air for some minutes in an NMR tube, resonances attributable to the cyclic selenite of ethylene glycol became apparent in terms of ^{1}H, ^{13}C, and ^{77}Se NMR spectra.

DFT results and NBO analyses

Geometry optimization was performed at the B3LYP/6-31+G(2d,p) level of theory. Frequency analyses for both optimized structures did not show imaginary frequencies below $-6\ cm^{-1}$. The calculated bond lengths and angles are consistent with the experimental data from the X-ray structure analyses. Numerical data are given in Table 1.

An analysis of the bonding situation reveals practically identical results for **1** and **2**. Therefore the following discussion is based on the values of the ethylene glycol derivative **1** only. In a molecular-orbital approach, axially oriented O and Se p orbitals contribute to several canonical MOs in the sense of a 4e-3c bond. An MO associated with the Se lone pair is characterized by a dominant contribution of the Se 4s AO.

Table 1 Comparison of selected average experimental bond lengths and angles (XRD) for $Se(C_2H_4O_2)_2$ (**1**) and $Se(C_6H_{12}O_2)_2$ (**2**) [7] with the corresponding parameters calculated at the B3LYP/6-31+G(2d,p) level of theory.

	1		**2**	
	XRD	DFT	XRD	DFT
d(Se-O_{ax})/Å	1.87	1.87	1.87	1.87
d(Se-O_{eq})/Å	1.79	1.81	1.78	1.80
<(O_{ax}-Se-O_{ax})/°	167.8	167.7	165.8	166.7
<(O_{ax}-Se-O_{eq})/°	86.0	86.2	86.0	86.1
<(O_{eq}-Se-O_{eq})/°	103.9	103.0	110.0	107.4

Similar results were obtained by using a localized approach. In the framework of natural bond orbital (NBO) analysis [9], the Se-O bonds are markedly heteropolar, the relatively small contribution of the Se orbitals being dominated by 4p AOs. Thus the equatorial bonds (23 % Se character) resemble a $s^{0.08}p^{0.81}d^{0.11}$ hybridization, whereas a $s^{0.08}p^{0.68}d^{0.25}$ hybridization is assigned to the still more polar axial bonds (16 % Se character). In agreement with the MO approach, the lone pair on selenium is found to show a $s^{0.76}p^{0.24}$ hybridization. The d-AO contribution to the hybrid orbitals stems exclusively from low-populated Rydberg orbitals which − in conjunction with the highly ionic character of the Se-O bonds − leads to no actual valence-shell d-orbital occupation. Accordingly, a natural population analysis (NPA) reveals an overall Se-AO contribution where the d participation does not exceed a value that might be expected if diffuse functions are provided ($s^{1.70}p^{2.29}d^{0.04}$).

Figure 2 shows isocontour plots of selected natural orbitals. As expected, the axial 4e-3c-bond region can not be treated as straightforward in the localized NBO approach, as the equatorial bonds which better tolerate a 2e-2c formalism. Thus a second-order-perturbation-theory analysis reveals that there are energetically favorable $\sigma-\sigma^*$ interactions (negative hyperconjugation) between occupied Se-O bonding orbitals and the adjacent antibonding Se-O orbitals. As expected, due to their approximated collinearity, the two possible interactions between an axial bonding (b) and the opposed antibonding Se-O orbitals (d) give rise to the largest two-electron stabilization energies, which are

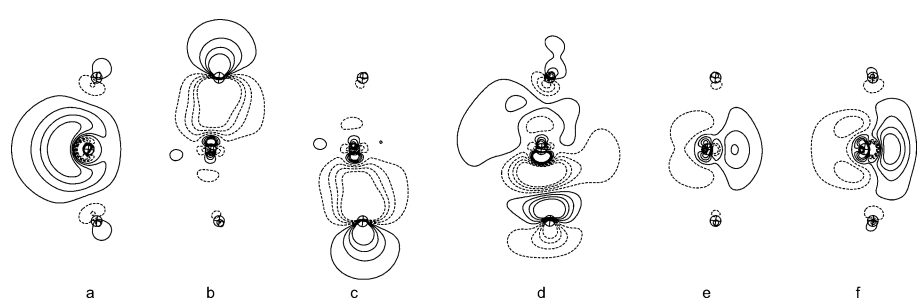

Figure 2 Isocontour plots of selected natural bond orbitals in **1**. Isolines are drawn at 0.03, 0.08, 0.13 and 0.18. The drawing plane contains both axial oxygen atoms and the central selenium atom (crossed circles). (a) lone pair on Se, (b, c) Se-O_{ax} bonding s orbitals, (d) Se-O_{ax} antibonding σ^* orbital, (e) Se-O_{eq} bonding s orbitals, (f) Se-O_{eq} antibonding σ^* orbitals.

349 kJ mol^{-1}. The corresponding energy for each of the four possible interactions between equatorial Se-O bonds (e) and antibonding axial orbitals (d) is 234 kJ mol^{-1}. The third possible type of interaction, which gives rise to two-electron stabilization energies of 180 kJ mol^{-1}, is a delocalization from axial bonding Se-O orbitals (b, c) to equatorial antibonding orbitals (f). The marked stereochemical activity of the slightly decentered lone pair (a) on selenium is obvious.

As a result, the bonding situation in **1** might be described by assuming a nearly non-hybridized Se atom forming two 2e-2c Se-O bonds to the O atoms in the equatorial plane and a 4e-3c Se-O bond along the linear O-Se-O fragment. The lone pair is located mainly in the Se 4s orbital but is decentered by a considerable 4p contribution. Accordingly, the O_{ax} atoms are bent away from the thus weakly stereochemically active Se lone pair.

Conclusions

The X-ray analysis of 1,4,6,9-tetraoxa-5λ^4-selena-spiro-[4.4]nonane provides information about the metrical properties of the coordination environment and the bonding of the selenium atom. An NBO treatment shows the highly heteropolar character of the Se-O bonds and the dominant s character of the selenium lone pair. With this structural knowledge at hand, the optimum O-atom pattern that has to be provided by a chelating carbohydrate ligand can be derived.

References

[1] R. R. Holmes, *Acc. Chem. Res.* **1998**, *31*, 535−542.
[2] R. R. Holmes, *Acc. Chem. Res.* **2004**, *37*, 746−753.
[3] S. D. Lahiri, G. Zhang, D. Dunaway-Mariano, K. N. Allen, *Science* **2003**, *299*, 2067−2071.
[4] D. Behne, H. Weiler, A. Kyriakopoulos, *J. Reprod. Fertil.* **1996**, *106*, 291−297.
[5] R. Paetzold, M. Reichenbächer, *Z. Chem.* **1970**, *10*, 307−308.
[6] D. B. Denney, D. Z. Denney, P. J. Hammond, Y. F. Hsu, *J. Am. Chem. Soc.* **1981**, *103*, 2340−2347.
[7] R. O. Day, R. R. Holmes, *Inorg. Chem.* **1981**, *20*, 3071−3075.
[8] M. J. Frisch, G. W. Trucks, H. B. Schlegel, G. E. Scuseria, M. A. Robb, J. R. Cheeseman, J. A. Montgomery, Jr., T. Vreven, K. N. Kudin, J. C. Burant, J. M. Millam, S. S. Iyengar, J. Tomasi, V. Barone, B. Mennucci, M. Cossi, G. Scalmani, N. Rega, G. A. Petersson, H. Nakatsuji, M. Hada, M. Ehara, K. Toyota, R. Fukuda, J. Hasegawa, M. Ishida, T. Nakajima, Y. Honda, O. Kitao, H. Nakai, M. Klene, X. Li, J. E. Knox, H. P. Hratchian, J. B. Cross, V. Bakken, C. Adamo, J. Jaramillo, R. Gomperts, R. E. Stratmann, O. Yazyev, A. J. Austin, R. Cammi, C. Pomelli, J. W. Ochterski, P. Y. Ayala, K. Morokuma, G. A. Voth, P. Salvador, J. J. Dannenberg, V. G. Zakrzewski, S. Dapprich, A. D. Daniels, M. C. Strain, O. Farkas, D. K. Malick, A. D. Rabuck, K. Raghavachari, J. B. Foresman, J. V. Ortiz, Q. Cui, A. G. Baboul, S. Clifford, J. Cioslowski, B. B. Stefanov, G. Liu, A. Liashenko, P. Piskorz, I. Komaromi, R. L. Martin, D. J. Fox, T. Keith, M. A. Al-Laham, C. Y. Peng, A. Nanayakkara, M. Challacombe, P. M. W. Gill, B. Johnson, W. Chen, M. W. Wong, C. Gonzalez, J. A. Pople, *Gaussian 03, Revision B.03/D.01.*, Gaussian, Inc., Wallingford CT, **2004**.
[9] E. D. Glendening, J. K. Badenhoop, A. E. Reed, J. E. Carpenter, J. A. Bohmann, C. M. Morales, and F. Weinhold, *NBO 5.G*, Theoretical Chemistry Institute, University of Wisconsin, Madison, **2001**.
[10] A. Altomare, M. C. Burla, M. Cavalli, G. L. Giacovazzo, A. Gagliardi, A. G. G. Moliterni, G. Polidori, R. Spagna, *SIR97, A New Tool For Crystal Structure Determination and Refinement*, *J. Appl. Cryst.* **1997**, *30*, 565.
[11] G. M. Sheldrick, *Acta Crystallogr.* **2008**, *A64*, 112−122.
[12] M. N. Burnett, C. K. Johnson, *ORTEP III, Oak Ridge Thermal Ellipsoid Plot Program for Crystal Structure Illustrations*, Oak Ridge National Laboratory Report ORNL-6895, **1996**.
[13] D. Cremer, J. A. Pople, *J. Am. Chem. Soc.* **1975**, *97*, 1354−1358.

